Comparative Analysis of Support Vector Machine for Hyper spectral Image Classification

Komathi.B.J[1], Dr.R.Gayathri[2]
[1]*PG Student, Department of ECE, Sri Venkateswara College of Engineering, Tamilnadu 602117*
[2]*Associate Professor, Department of ECE, Sri Venkateswara College of Engineering, Tamilnadu 602117*

***Abstract*- Hyperspectral image (HSI) classification is a very important subject in the area of remote sensing. In common, the intricate distinctiveness of hyperspectral data makes the precise classification of such data difficult for traditional machine learning methods. In addition, hyperspectral imagery often deals with an innately nonlinear relationship between the spectral information captured and therefore the corresponding materials. Machine learning has been acknowledged as a robust feature extraction tool to successfully address nonlinear issues and widely used in image processing tasks. This survey paper presents a scientific review of machine learning-based HSI classification using Graph-cut and Local Covariance Matrix Representation (LCMR) method and compares various strategies for this topic. Specifically, we first summarize the foremost challenges of HSI classification which cannot be effectively overcome by traditional methods, and also introduce the advantages of Support Vector Machine (SVM) model to handle these problems. Experimental results have been conducted using publicly available hyperspectral data sets for classification.**

***Index terms*- Hyperspectral images, graph cut, Covariance matrix representation (CMR), Support Vector Machine (SVM), feature extraction, hyperspectral image (HSI).**

I.INTRODUCTION

The "hyper" in hyperspectral signifies "over" as in "too much" and which is alluding to the enormous number of estimated frequency groups from the noticeable to the infrared scope of the electromagnetic range. The data gathered over these spectral bands is known as hyperspectral information which can be utilized to distinguish and figure an enormous scope of materials which are frightfully comparable and those can't be recognized by multispectral pictures. The material of structures cannot recognize objects which are made up with a similar material yet with not at all like semantic implications with the assistance of multispectral images. The surface of certain structures and the streets can be made by a similar material and those can be recognized by hyperspectral information. So relevant data, geometrical highlights of hyperspectral image are required to distinguish an image appropriately [1]. The principle complexity in estimation of logical data lies in the high dimensions of spectral channels.

Hyperspectral images are not just used to recognize various classes of land spread, yet additionally the characterizing parts of each land spread classification, for example, minerals, and soil and vegetation type and so forth [2]. Remotely detected hyperspectral imaging permits the examination of pictures inside and out. This investigation can be valuable in different regions. Fig1 delineates the application regions of hyperspectral imaging.

Based on the recent studies published in [6], HSI arrangement (i.e., appointing every pixel to one certain class dependent on its spectral attributes) is the most energetic field of research in the hyperspectral network and has drawn wide interest in the remote sensing field. In HSI classification undertakings, there exist two fundamental difficulties: 1) the huge spatial fluctuation of spectral signatures and 2) the constrained accessible training sample versus the high dimensionality of hyperspectral information. The main challenge is frequently brought by numerous components, for example, changes in illumination, natural, atmospheric, and fleeting conditions. The ensuing test will achieve severely introduced issues for specific procedures and diminishes the hypothesis limit of classifiers.

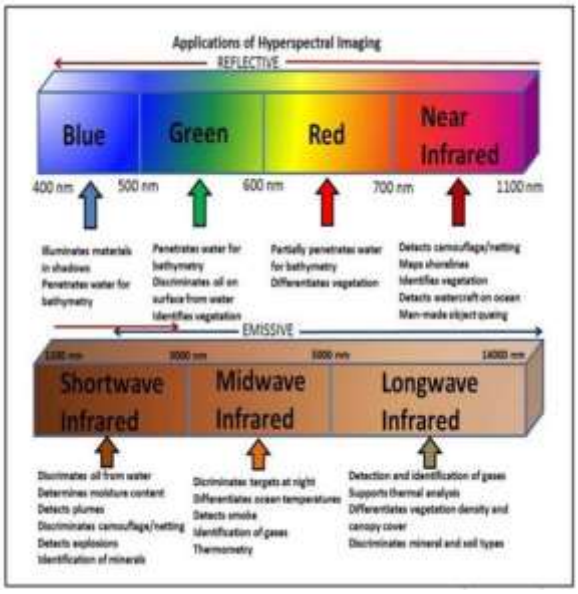

Figure 1. Applications of Hyperspectral Imaging

The goal of image classification methods is to consequently characterize all pixels in the image into land spread classes. The two fundamental difficulties stand up to during arranging hyperspectral images, initial one is a curse of dimensionality which is likewise named as Hughes phenomenon and another is working with samples which are less trained. In light of the utilization of training samples can be made into regulated, unsupervised and semi-administered hyperspectral image characterization strategies. In directed classification just marked data is utilized to train the classifier. In unaided strategy the PC or calculation naturally bunches pixels with comparable spectral attributes (implies, standard deviations, and so forth) into one of a kind groups as indicated by some factually decided models. While in semi-supervised classification both named and unlabeled information can be utilized to prepare the classifier. In this paper, LCMR and graph cut methods are portrayed to deal with the issues, for example, high dimensionality and working with the restricted training samples. Additionally, talks about issues identified with every strategy and possibilities to direct classification. The remainder of the paper is structured in following manner.

II. LCMRMETHODFORCLASSIFICATIONOFHIS

Fig. 2 shows the flowchart of the proposed method for the classification of HSIs, which consists of the following three steps. First, for each pixel, the local neighboring pixels on the subspace (e.g., the MNF-based dimensionality reduced subspace) are obtained using the cosine distance. Then, the CMR is applied on each pixel and its local neighboring pixels on the subspace. Finally, the obtained covariance matrices are used as spatial–spectral features and fed into an SVM with Log Euclidean-based kernel for label assignment.

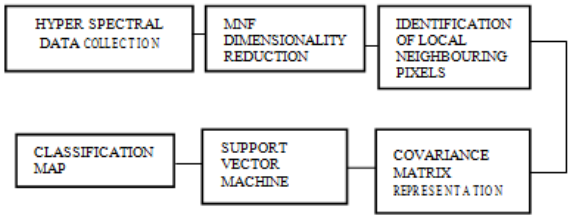

Fig. 2. Flowchart of the proposed LCMR classification method

A. *Spectral Dimensionality Reduction*

In order to reduce the computational complexity and discard noise, the MNF [18] is first applied to the original HSI. Specifically, given an HSI Z $R^{I\times J\times K}$, the dimensionally reduced HSI F $\epsilon R^{I\times J\times L}$can be obtained with (2), where I and J denote the size of two spatial dimensions, K is the size of the spectral dimension, and L represents the number of MNF components. Note that, Z is vectorized to a matrix along the spectral dimension at first and the inverse procedure of vectorization is conducted to obtain F. Compared with other transform-based dimensionality reduction methods (e.g., PCA [16] and ICA [17]), the main advantage of the MNF is that noise can be effectively removed on the MNF transformed space, since the MNF aims at maximizing the SNR.

B. *Identification of Local Neighboring Pixels*

Using a square window of fixed size is a common way to explore the spatial information for the HSI classification. However, it should be noted that there may still be some pixels with low spectral correlation within the window, especially around the object edges. To address this issue, we introduce a local neighboring pixels construction method to discard the dissimilar neighboring pixels in the reduced subspace.

First, a large window with size T × T is used to extract the neighbors with regard to a central pixel denoted byf_1^j, where the neighboring pixels are denoted by $\{f_i^j\}_{i=2,\ldots,T_2}$

j= 1,...,N. N is the total number of pixels in the image. The K-NN method with the cosine distance is applied on these pixels, i.e., the $\{f_1^j\}$ and its $T_2 - 1$ neighboring pixels, i.e., $\{f_i^j\}_{i=2,\ldots,T_2}$. The cosine distance between the central pixel and its neighboring pixels is calculated as follows:

$$\cos(f_1^j, f_i^j) = \frac{(f_1^j, f_i^j)}{||f_1^j||_2 \cdot ||f_i^j||_2} (1)$$

Where $<\cdot>$ and $\|\cdot\|$ denote the inner product and the Frobenius norm, respectively. Only the K − 1 most similar pixels with regard to the central pixel within the window are taken into consideration, whereas the rest of them are discarded. In this way, we can construct a local neighborhood for each test pixel, i.e.,$\{f_k^j\}_{k=1,\ldots,K}$ Obviously, the selected K − 1 pixels are not only spatially close to the central pixel but also share relatively similar spectral information which can be used to extract more discriminative features in the construction of CMRs. At this point, it is important to emphasize that the cosine distance-based K-NN strategy is used in our method because of the following two reasons. First, it is quite common to use the cosine distance-based similarity measurement for HSI data processing and it has been reported to specifically provide a good performance in the HSI classification. Second, although there are some shape adaptive based methods which can automatically search for similar pixels that show a good performance on the HSI classification and denoising, they need careful parameter setting. In addition, these methods exhibit heavier computational burden. Overall, to make the proposed method simple yet effective, the cosine distance-based K-NN is adopted in our method.

C. Construction of CMRs for Each Pixel and Its Local Neighbors

After obtaining $\{f_k^j\}_{k=1,\ldots,K}$ it is easy to construct the CMR for the central pixel f j 1 with (3), which can be rewritten asfollows:

$$C_j = \frac{1}{K-1} \sum_{k=1}^{K} (f_k^j - \mu)(f_k^j - \mu)^T (2)$$

Where, μ denotes the mean vector of the set of feature vectors$\{f_k^j\}_{k=1,\ldots,K}$. By conducting this process, a set of covariance matrices are extracted for each of the pixels in the image, i.e., $\{C_j\}_{j=1,\ldots,N}$.The covariance matrices sets are then used as spatial–spectral features and fed into an SVM with Log Euclidean based kernel for final classification

The well-known Airborne Visible/Infrared Imaging Spectrometer (AVIRIS) Indian Pines scene is used for illustrative purposes. As can be seen from the first row in Fig. 3, the four pixels exhibit very similar spectral signatures, although they belong to different classes (i.e., grass-pasture-mowed, corn, soybean mintill, and soybean- clean). As a result, it is very challenging to discriminate these pixels. The normalized distance among the four pixels both on the OSS and the MS is reported in Table I. As can be seen, the total normalized distance among the four pixels in the OSS is 0.0097, whereas the total distance among the four pixels in the MS is 0.2742. Obviously, the CMR can enlarge the distance among the four pixels (with very similar spectral signatures but actually belonging to different classes).

III. GRAPH CUT METHOD FORCLASSIFICATION

An input B-band hyperspectral image can be represented as a set of n pixel vectors $X=\{x_i \epsilon R^B, i=1,2,\ldots,n\}$. The goal is to compute a classification map L = {L_i,i = 1, 2,...,n}, where each pixel xi is assigned to one of K information classes $\{\omega_1, \omega_2, \ldots, \omega_k\}$, i.e., has a class label Li.The proposed SVM-GC method comprises two main phases (see Fig. 1):

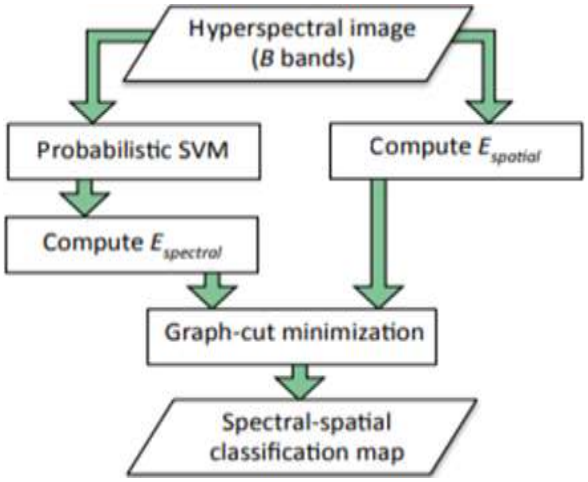

Fig.3. Flowchart of the proposed SVM-GC classification method[5]

A. Probabilistic pixel wise classification

The first phase consists in estimating class probabilities for each pixel {p(L_i = k|x_i), k = 1, ..., K}, i = 1, 2, ..., n. We propose to utilize a probabilistic SVM classifier, which performs better and has been generally applied to investigate hyper spectral information [4, 6, 7]. We refer the reader to [7] for details about estimation of class probabilities by pairwise coupling of binary probability estimates.

B. Graph-cut energy minimization

In this phase, the spectral-spatial classification map is computed by minimizing energy of the form:

$$E(L) = E_{data}+E_{smooth}= \sum_{i=1}^{n} V_i\,(L_i)+\sum_{i\sim j}^{n} W_{i,j}\,(L_i, L_j)$$

Where individual potentials Vi(Li) measure a penalty for a pixel i to have a label L_i,i∼j denotes a pair of spatially adjacent pixels (eight-neighborhood is used in our work), and $W_{i,j}(L_i , L_j)$ are interaction terms between neighboring pixels i and j expressing spatial coherency

The individual potentials are computed by using the estimated class probabilities for each pixel:

$V_i(L_i) = -\ln(p(L_i|x_i))$

To compute spatial interaction terms, most studies on remote sensing image analysis employ a Pottsmodel

$W_{i,j}\,(L_i,L_j) = \beta(1-\delta(L_i,L_j))$

Where δ(·) is the Kronecker function (δ(a, b) = 1 for a = b and δ(a, b) = 0 otherwise) and β is a positive constant parameter that controls the importance of spatial smoothing. This model will in general break down grouping results at the edges between land-spread classes and close to small-scale details.

In order to preserve the borders in the classification map, "edge" functions have been proposed and integrated in the spatial energy term

$$W_{i,j}\,(L_i,L_j) = \beta(1-\delta(L_i,L_j))\,\frac{t}{t+|\rho_{i|j}|}$$

Where,$\rho_{i|j}$ is the gradient value of the pixel i in the direction of j, and t is a parameter controlling the fuzzy edge threshold. In this paper, we further investigate how to correctly incorporate the information associated with class edges within the MRF framework. We express the spatial interaction term as a function of dissimilarity between spectra of the adjacent pixels:

$W_{i,j}\,(L_i,L_j) = \beta(1-\delta(L_i,L_j))\,\exp|-d(x_i,x_j)|$

Where, $d(x_i,x_j)$ measures the discrepancy between the pixel vectors $x_i = (x_{i1},\dots,x_{iB})^T$ and $x_j = (x_{j1},\dots,x_{jB})^T$. We explored the use of three dissimilarity measures

1. L2-normbased:

$$d_{L2}(x_i,x_j) = \frac{\sum_{b=1}^{B}|(x_{ib}-x_{jb})^2|}{2\sigma^2\,B}$$

Where σ is a standard deviation of the image spectral values.

2. The SAM distance computes the angle between spectral vectors:

$$d_{SAM}(x_i,x_j) = \arccos\frac{\sum_{b=1}^{B} x_{ib}x_{jb}}{\sum_{b=1}^{B} x_{jb}^2{}^{\frac{1}{2}}\sum_{b=1}^{B} x_{jb}^2{}^{\frac{1}{2}}}$$

3.The SID-based measure computes the discrepancy of probabilistic behaviors between the spectral signatures of two pixels:

$$d_{SID}\ (x_i,x_j) = \frac{1}{B}+\sum_{b=1}^{B}\left(q_b(x_i)\log\frac{q_b(x_i)}{q_b(x_j)}+ q_b(x_j)\log\frac{q_b(x_j)}{q_b(x_j)}\right)$$

Where

$$q_b(x_i) = \frac{x_{ib}}{\sum_{i=1}^{B} x_{il}}$$

The resulting energy E(L) is minimized by applying the efficient α-expansion graph-cut-based algorithm described.

IV. EXPERIMENTAL RESULTS ANDDISCUSSION

A. Pavia Dataset:

In the proposed method PAVIA dataset is used. The University of Pavia image was acquired by the ROSIS-03 sensor over the campus at the University of Pavia, Italy. This data set contains 103 spectral bands after the noise- corrupted bands are discarded, and each band is of size 610×340. The spatial resolution of this data set is 1.3 m, and the spectral coverage ranges from 0.43 to 0.86 μm.. Image ground truths differentiate 9 classes each.

Ground truth classes for the Pavia dataset and their respective sample numbers are given in the table as follows. The RGB or 3- band image and the ground truth of the PAVIA dataset is obtained as shown in the figure 4. "Ground truth" refers to information collected on location. Ground truth also helps with atmospheric correction.

S. No	CLASSES	SAMPLES
1	Asphalt	6631
2	Meadow	18649
3	Gravel	2099
4	Trees	3064
5	Painted metal sheets	1345
6	Bare soil	5029
7	Bitumen	1330
8	Self-blocking bricks	3682
9	Shadows	947

Table 1: Ground truth classes of PAVIA Dataset

Fig 4: RGB and ground truth image of PAVIA dataset

The classification result of the Hyperspectral image using the SVM-Graph cut method is obtained as in the figure

Fig 5: Classification result of SVM-Graph cut method

The above classification result is satisfactory but noisy due to insufficient training samples and in this method only the spectral parameters are considered, we can further improve the results by considering both Spatial-Spectral parameters along with SVM-LCMR method. The classification results of the spatial-spectral feature extraction of Hyperspectral images using SVM-LCMR is obtained as in figure

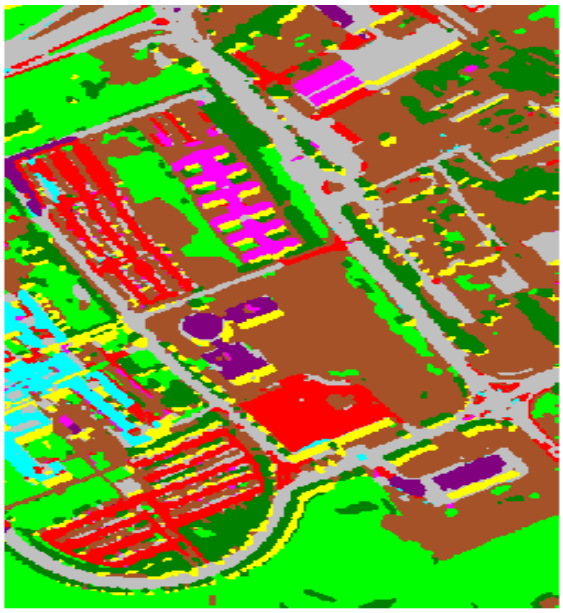

Fig 6: Classification result of SVM-LCMR method

Inference from the figure 6 is that all the nine classes of the PAVIA dataset are classified and the classification accuracy is better when compared with the previous SVM-Graph cut. The accuracy comparison for both the methods are listed in the table 2

ACCURACY CALCULATION	SVM USING GRAPH CUT METHOD	SVM USING LCMR
OVERALL ACCURACY (OA)	79.8%	84.18%
AVERAGE ACCURACY (AA)	80.2%	84.94%

Table 2: Comparison of accuracy between SVM-Graph cut method and SVM-LCMR method

From the table 6.2, The Average Accuracy (AA) is the average of the accuracies for each class and Overall Accuracy (OA) is the accuracy of each class weighted by the proportion of test samples for that class in the total training set. The Overall Accuracy is 84.18% for LCMR method and 79.8% for Graph cut method and the Average Accuracy is 84.94% for LCMR and 80.2% for graph cut method. Therefore, the Local Covariance Matrix Representation (LCMR) method can outperform other state- of-the-art methods in terms of qualitative and quantitative

performance, especially when the number of training samples is minimum.

V. CONCLUSION

Traditional machine learning techniques utilized in HSI classification depend on the way that various materials display distinctive spatial-spectral curve and process every pixel freely. Machine learning algorithms generally utilized in HSI characterization field incorporate k-nearest neighbor (KNN), linear discriminant analysis (LDA), decision tree, random forest, support vector machines (SVM) and so on. Among these methods, SVM is considered a benchmark method since it can handle the ‘‘curse of dimensionality’’ problem and requires a relatively small size of training samples. In spite of the fact that the pixel-wised classification techniques can utilize every pixel's spectral data, the acquired results can in any case be noisy. This is principally in light of the fact that the spatial data has not been used completely. Truth be told, the spatial feature is similarly significant as the spectral feature and can be utilized to improve the classification exactness. So, The SVM along with Linear Covariance Matrix Representation is used which has given good classification results with a smaller number of training samples. The Convolutional Neural Networks (CNN) can be used for the classification of HSI. CNN could lessen the chance of getting unseemly spatial data, for example, noise contaminated sample or samples from different classes so the classification precision can be significantly improved.

REFERENCES

[1] Bing Liu, Xuchu Yu, Pengqiang Zhang, Anzhu Yu, Qiongying Fu, and Xiangpo Wei, “Supervised Deep Feature Extraction for Hyperspectral Image Classification”, IEEE Transactions on Geoscience and Remote Sensing, Vol.56, Issue:4, April 2018

[2] Shaohui Mei, Jingyu Ji, Junhui Hou, Xu Li and Qian Du “Learning Sensor-Specific Spatial-Spectral Features of Hyperspectral Images via Convolutional Neural Networks” IEEE Transactionson Geoscience and Remote Sensing, Vol.55, Issue:8, Aug 2017

[3] Wei Li, Guodong Wu, Fan Zhang and Qian Du “Hyperspectral Image Classification Using Deep Pixel-Pair Features”, IEEE Transactions on Geoscience and Remote Sensing, Vol.55, Issue:2, Feb2017

[4] Jiaojiao Li, Xi Zhao, Yunsong Li, Qian Du, Bobo Xi, and Jing Hu “Classification of Hyperspectral Imagery Using a New Fully Convolutional Neural Network”, IEEE Geoscience and Remote Sensing Letters, Vol.15, Issue:2, Feb 2018

[5] Y. Tarabalka and A. Rana, "Graph-cut-based model for spectral-spatial classification of hyperspectral images," 2014 IEEE Geoscience and Remote Sensing Symposium, Quebec City,QC,2014,pp.3418-3421

[6] Wenzhi Zhao and Shihong Du “Spectral–SpatialFeature Extraction for Hyperspectral Image Classification: A Dimension Reduction and Deep Learning Approach”, IEEE Transactions on Geoscience and Remote Sensing, Vol.54, Issue:8, Aug 201637

[7] PedramGhamisi, Yushi Chen and Xiao Xiang Zhu “A Self Improving Convolution Neural Network for the Classification of Hyper spectral Data” IEEE Geoscience and Remote Sensing Letters, Vol.13, Issue: 10, Oct2016

[8] Pietro Guccione, Luigi Mascolo, and Annalisa Appice “Iterative Hyperspectral Image Classification Using Spectral–Spatial Relational Features”, IEEE Transactions on Geoscience and Remote Sensing, Vol.53, Issue:7, July2015

[9] Yuliya Tarabalka, Jon AtliBenediktsson and Jocelyn Chanussot “Spectral–Spatial Classification of Hyperspectral Imagery Based on Partitional Clustering Techniques”, IEEE Transactions on Geoscience and Remote Sensing,Vol.47, Issue:8, Aug 2015

[10] Hong Li, Guangrun Xiao, Tian Xia, Y. Y. Tang, and Luoqing Li “Hyperspectral Image Classification Using Functional Data Analysis”, IEEE Transactions on Cybernetics, Vol.15, Issue:9, Oct2014

[11] M. Moroni, E. Lupo, E. Marra, and A. Cenedese, ‘‘Hyperspectral image analysis in environmental monitoring: Setup of a new tunable filter platform,’’ Procedia Environ. Sci., vol. 19, pp. 885–894, Jan.2013.

[12] Y.-Z. Feng and D.-W. Sun, ‘‘Application of hyperspectral imaging in food safety inspection and control: A review,’’ Critical Rev. FoodSci. Nutrition, vol. 52, no. 11, pp. 1039–1058,2012.

[13] S. Delalieux, B. Somers, B. Haest, T. Spanhove, J. V. Borre, and C. Mücher, ‘‘Heathland conservation status mapping through integration of hyperspectral mixture analysis and decision tree classifiers,’’ RemoteSens. Environ., vol. 126, pp. 222–231, Nov. 2012 38

[14] P.Ghamisi, J.A.Benediktsson, and J.R.Sveinsson, ‘‘Automatic spectral– spatial classification framework based on attribute profiles and supervised feature extraction,’’ IEEE Trans. Geosci. Remote Sens., vol. 52, no. 9, pp. 5771–5782, Sep.2014.

[15] L.WeiandD.Qian, ‘‘An efficient spatial-spectral classification method for hyperspectral imagery,’’Proc.SPIE,vol.9124,May2014,Art.no.912410.

[16] Y.Chen, X.Zhao, and X.Jia, ‘‘Spectral–spatial classification of hyperspectral data based on deep belief network,’’ IEEE J. Sel. Topics Appl. Earth Observ. Remote Sens., vol. 8, no. 6, pp. 2381–2392, Jun.2015.

[17] Y. Liu, G. Cao, Q. Shen, and M. Siegel, ‘‘Hyperspectral classification via deep networks and super pixel segmentation, ’’Int.J. Remote Sens., vol.36, no. 13, pp. 3459–3482, Jul.2015.

[18] W.Hu, Y.Huang, L.Wei, F.Zhang, and H.Li, ‘‘Deep convolutional neural networks for hyperspectral image classification,’’ J. Sensors, vol. 2015, Jan. 2015, Art. no. 258619.

[19] K. Makantasis, K. Karantzalos, A. Doulamis, and N. Doulamis, ‘‘Deep supervised learning for hyperspectral data classification through convolutional neural networks,’’ in Proc. IEEE Int. Geosci. Remote Sens. Symp. (IGARSS), Jul. 2015, pp.4959–4962.

[20] X. Ma, J. Geng, and H. Wang, ‘‘Hyperspectral image classification via contextual deep learning,’’ EURASIP J. Image Video Process., vol. 2015, no. 1, p. 20, Dec.2015.